

## Electronic Supplementary Information (ESI)

### Organotitanias: A versatile approach for band gap reduction in titania based materials

Marisa Rico-Santacruz,<sup>1</sup> Ángel E. Sepúlveda,<sup>b</sup> Elena Serrano,<sup>1</sup> Elena Lalinde,<sup>2</sup> Jesús R. Berenguer,<sup>2\*</sup>, Javier García-Martínez<sup>1\*</sup>

<sup>a</sup>Laboratorio de Nanotecnología Molecular. Departamento de Química Inorgánica. Universidad de Alicante, Carretera San Vicente s/n, E-03690, Alicante, Spain. Fax: +34 965903454; Tel: +34 965903400 ext.2224; E-mail: [j.garcia@ua.es](mailto:j.garcia@ua.es), URL: [www.nanomol.es](http://www.nanomol.es)

<sup>b</sup> Departamento de Química-Centro de Investigación en Síntesis Química (CISQ), Universidad de La Rioja, Madre de Dios, 51, E-26006, Logroño, Spain. URL: <https://cisq.unirioja.es/gmmo.php> Fax: +34 941299621; Tel: +34 941299646; E-mail: [jesus.berenguer@unirioja.es](mailto:jesus.berenguer@unirioja.es)

#### 1. Experimental section: general methods

IR spectra were recorded on a Nicolet Nexus FT-IR Spectrometer in a wavenumber range from 4000 to 200 cm<sup>-1</sup>. All samples were prepared as KBr pellets. Elemental analyses were carried out with a Thermo Finnigan Flash 1112 microanalyzer at 900 °C, using high purity helium as carrier gas. Samples were weighted in tin capsules with vanadium pentoxide (V<sub>2</sub>O<sub>5</sub>) for helping the combustion. The standard used for the quantitative determination of the organic compound incorporated contained 0.45 wt% N, 10.03 wt% C, 1.30 wt% H and 0.00 wt% S. The values given for each sample are the average of four experiments. Mass spectra were recorded on a Microflex MALDI-TOF Bruker (MALDI) spectrometer operating in the linear and reflector modes using dithranol as the matrix. Thermogravimetric analyses were carried out in a Mettler Toledo TG-ATD (TGA/SDTA851e/sf/110). The measurements were carried out under nitrogen/oxygen atmosphere (4:1) from room temperature to 900 °C, with a heating rate of 10 °C min<sup>-1</sup>.

X-ray Photoelectron Spectroscopy (XPS) was carried out in a VG-Microtech Multilab instrument, using MgK-alpha radiation of energy 1253.6 eV and pass energy of 50 eV. The analysis pressure during dta acquisition was 5x10<sup>-7</sup> Pa. A careful deconvolution of the spectra was made and the areas under the peaks were estimated by calculating the integral of each peak after subtracting a Shirley background and fitting the experimental peak to a combination of Lorentzian/Gaussian lines of 30-

70 % proportions. Binding energies were referenced to the C1s line at 284.6 eV from adventitious carbon.<sup>[1]</sup>

X-ray diffraction (XRD) analyses were carried out with a Bruker D8-Advance diffractometer (operating at 40 kV and 40 mA), using a CuK $\alpha$  radiation ( $\lambda = 1.54056 \text{ \AA}$ ). The samples were scanned from 20° to 60° ( $2\theta$ ), at a scanning velocity of 0.05 min<sup>-1</sup>. Domain size and anatase spacing ( $d_{101}$ ) of samples were calculated using Eq. Scherrer and Eq. Bragg, respectively.

The morphology of the mesoporous materials was investigated by transmission electron microscopy (TEM) using a JEM-2010 microscope (JEOL, 200 kV, 0.14 nm of resolution). Samples for TEM studies were prepared by dipping a sonicated suspension of the sample in ethanol on a carbon-coated copper. The digital analysis of the TEM micrographs was performed using Gatam DigitalMicrographTM 1.80.70 for GMS 1.8, being the particle size estimated as an average of the size of eighty particles. Similarly, anatase spacing ( $d_{101}$ ) calculated from TEM images using Gatam software.

Porous texture was characterized by N<sub>2</sub> adsorption at 77 K in an AUTOSORB-6 apparatus. The samples were previously degassed for 5 h at 373 K at 5x10<sup>-5</sup> bars. BET surface areas were estimated by using multipoint BET method, using the adsorption data in the relative pressure ( $P/P_0$ ) range of 0.05–0.30. The pore size distribution was calculated from the adsorption branch of the N<sub>2</sub> physisorption isotherms, using the Barret-Joyner-Halenda (BJH) method. As expected for these materials, the micropore volume, estimated from the t-plot method, was determined to be zero and thus the mesopore volume can be directly read from the isotherms at relative pressure of 0.95. These values are in good agreement with those obtained from the adsorption branch of the nitrogen isotherm using the BJH method, where the volume was measured at the plateau of the cumulative adsorption pore volume plot.

DRUV spectra were carried out in air at room temperature in the wavelength range 800-200 nm using a Shimadzu UV-2401 PC spectrophotometer with BaSO<sub>4</sub> as the reference material. For the

estimation of the band-gap, the reflectance data were converted into the equivalent absorption coefficient using the Kubelka-Munk formalism according to equation (1):

$$F(R') = [1-(R')]^2/2(R') \quad (1)$$

where  $R'$  is the reflectance value obtained directly from the spectrophotometer. Band gap calculations are based on the  $[F(R')hv]^{n/2}$  versus photon energy ( $h\nu$ ) plot (Tauc plots).<sup>[2-9]</sup>

Photocatalytic activity of the synthesized materials was evaluated by photocatalytic degradation of Rhodamine 6G molecules in aqueous solution under UV or visible radiation. For a typical UV light degradation test, an aqueous suspension of Rhodamine 6G ( $5 \times 10^{-5}$  M, 100 ml) with  $0.15 \text{ g L}^{-1}$  of as-synthesized catalyst was stirred during 30 min in the dark, to achieve the adsorption/desorption equilibrium of the dye on the catalyst surface. Afterwards, this suspension was irradiated with UV light using a photochemical reactor system with a 125W medium-pressure Hg lamp located in cooled, double-walled quartz, immersion well. The concentration of the dye was monitored by UV-Vis spectroscopy analysis in the 700-300 nm wavelength range, using a Jasco V-650 UV-vis or an Agilent 8453 spectrophotometers. As several intermediate species can appear during the photodegradation process, the total concentration of Rhodamine species was estimated based on the maximum absorbance observed in the 490 to 530 nm range. For the experiments under visible light, a similar procedure was followed, but using a 400W medium-pressure Hg lamp located in a double-walled Pyrex immersion well, cooled with a 2M solution of  $\text{NaNO}_2$  (UV cutoff filter  $> 400$  nm).

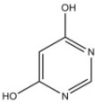
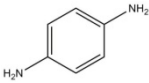
To further investigate the mechanism of the RhB degradation process under visible light using the photocatalyst  $\text{TiO}_2$ -PPD-b, controlled experiments have been carried out to determine the dominant active species involved in the photocatalytic reactions. The experimental procedure was similar to that described before, but using aqueous solutions of Rhodamine 6G ( $5 \times 10^{-5}$  M) with triethanolamine (TEOA,  $5 \times 10^{-2}$  M) or isopropanol (iPrOH,  $5 \times 10^{-2}$  M), which were used to scavenge photogenerated holes ( $h^+$ ) or hydroxyl radicals ( $\cdot\text{OH}$ ), respectively.<sup>[8]</sup>

For samples irradiated with UV light, a total organic carbon analyzer (TOC 500A, Shimadzu) was used in order to determinate the TOC content of the synthesized samples before and after bleaching of the sample. A calibration curve using Rhodamine 6G with different concentrations was used for determining TOC contents of samples.

## 2. Discussion

Table S1 lists the structure and name of the organic compounds used for the synthesis of the mesoporous organotitanias, as well as the molar ratio of the synthesis gel, wt% of organic compound (nominal and found) and the nomenclature used for samples.

**Table S1.** Nomenclature of the synthesized organotitanias, indicating the name and formula of the incorporated organic compound, as well as the nominal and real organic compound content.

Sample	Organic compound name incorporated	Organic compound formula	Org/TBOT molar ratio	Nominal Org. Cont. (wt%)	Org. cont. <sup>a)</sup> (wt%)	Inc. Yield <sup>a)</sup> (%)
TiO <sub>2</sub> -DHP-a	4,6- dihydroxypyrimidine		0.05	6.6	3.9	59
TiO <sub>2</sub> -DHP-b			0.10	12.3	5.1	41
TiO <sub>2</sub> -DHP-c			0.20	21.9	5.0	23
TiO <sub>2</sub> -PPD-a	p-phenylenediamine		0.05	6.3	5.2	83
TiO <sub>2</sub> -PPD-b			0.10	11.9	4.6	39
TiO <sub>2</sub> -PPD-c			0.20	21.3	9.2	43

<sup>a)</sup> Organic content and incorporation yield as determined by elemental analysis from the C content.

As indicated in the main paper, free *p*-phenylenediamine (PPD) is prone to autoxidation in aqueous media to give dark materials following the mechanism shown in Figure S1. In our hybrid organotitanias, however, slow oxidation of PPD within the gel lead to a mixture of aromatic imine species (oxidized *p*-phenylenediamine OPPD), yielding black titania materials.

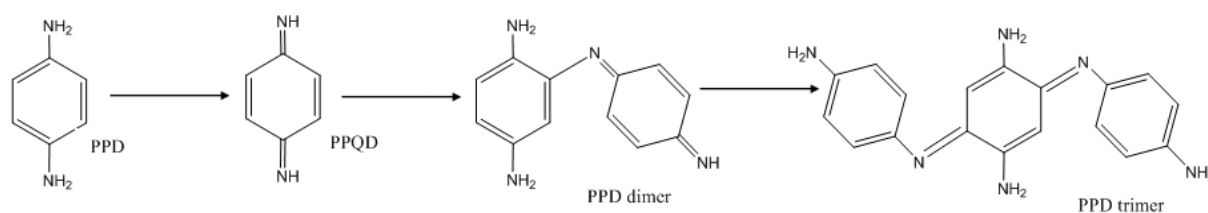


**Figure S1.** Oxidative process of free PPD in aqueous media.

Despite the different experiments described regarding the oxidation of PDD, we also tried to modify the extension of the oxidation process, making the reaction in several reducing or oxidizing media. For instance, the presence of  $\text{NaBH}_4$ , which does not react with PPD in the reaction conditions, led to the formation of a white solid material with structure of anatase, but the incorporation of organic moieties fell down drastically to negligible levels. Nevertheless, bubbling of air during the synthesis process yielded a similar black titania than that obtained carrying out the reaction in Ar atmosphere with deoxygenated water. Finally, prolonged refluxing of the black titania in EtOH or in aqueous solution of  $\text{NaBH}_4$  (24 to 48 h) only produces a slight decolouration of the material, which shows the enhanced hydrothermal stability of the organic species, probably due to their incorporation into the solid titania matrix.

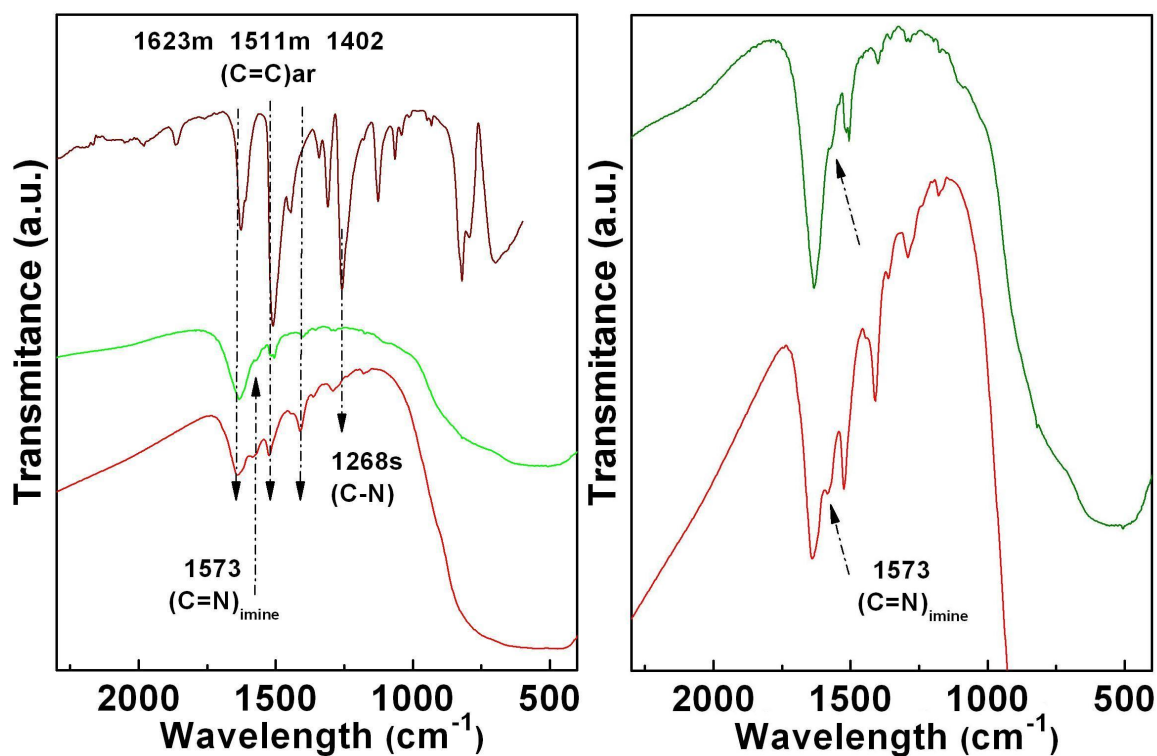


**Figure S2.** FTIR spectra of the black titania sample before, pale-grey gel precursor of black titania, namely Gel-TiO<sub>2</sub>-PPD-b, in green) and after the crystallization step (TiO<sub>2</sub>-PPD-b, in red).

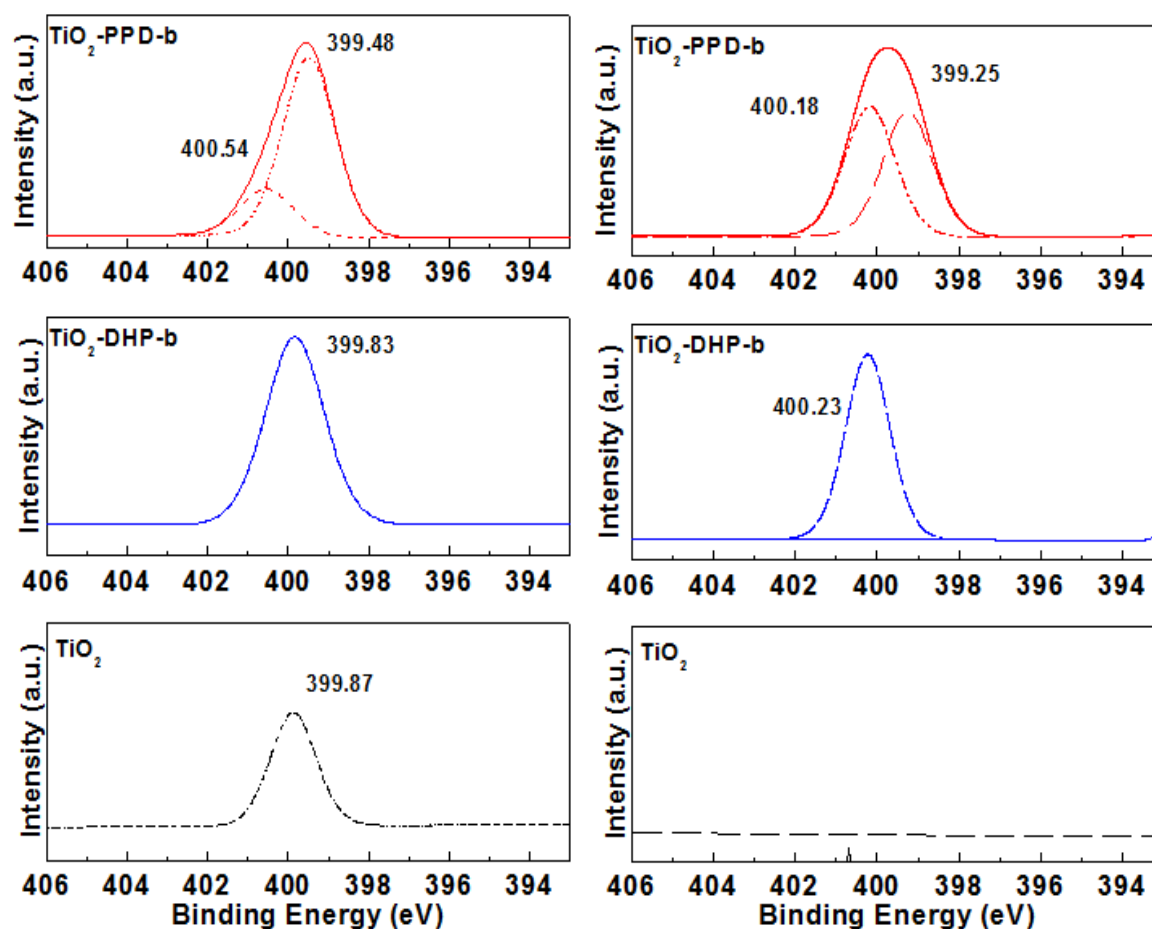


**Figure S3.** N 1s XPS spectra of hybrid  $\text{TiO}_2\text{-DHP-b}$  and  $\text{TiO}_2\text{-PPD-b}$  organotitanias before (left) and after (right) etching of samples during 20 s.

Nitrogen adsorption/desorption isotherms of the  $\text{TiO}_2\text{-DHP}$  and  $\text{TiO}_2\text{-PPD}$  organotitanias are shown in Figure S4. For comparison purposes, the isotherm of the organic-free  $\text{TiO}_2$  is also included. All materials show type IV isotherms with a similar shape, indicative of the mesoporous nature of these samples, being the textural properties similar to the organic-free titania. Furthermore, it cannot observe a significant effect of the ligand amount incorporated nor the type of ligand, in good agreement with the incorporation of the organic compounds in the framework of the titania and not between the titania nanoparticles.

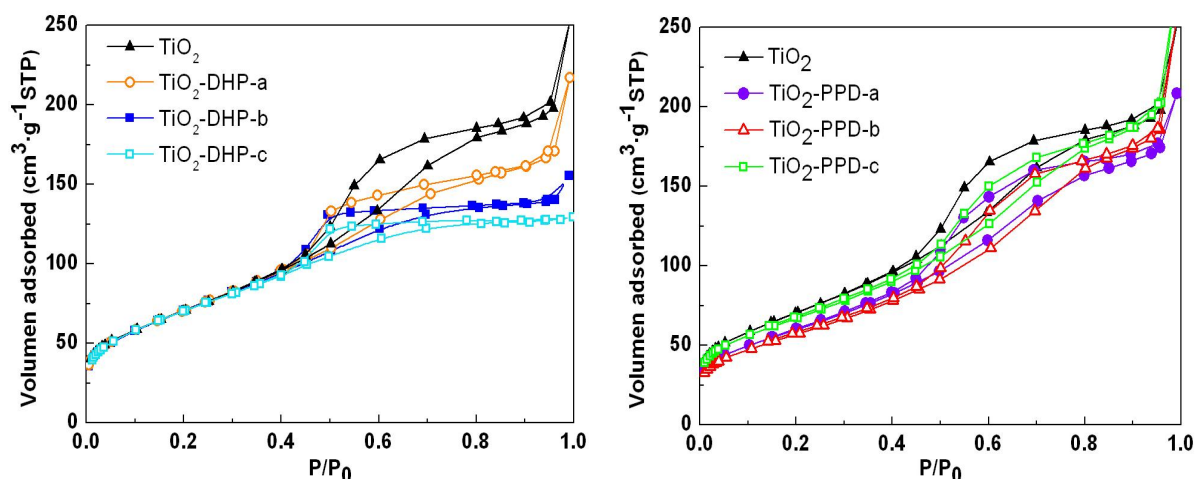


**Figure S4.** Nitrogen adsorption/desorption isotherms at 77 K of TiO<sub>2</sub>-DHP (left) and TiO<sub>2</sub>-PPD (right) organotitanias, as compared to the organic-free mesoporous titania TiO<sub>2</sub>.

XRD diffractograms of both TiO<sub>2</sub>-DHP and TiO<sub>2</sub>-PPD organotitanias, as well as the organic-free titania sample (Figure S5), show the characteristic peaks of the anatase structure, with a  $d_{101}$  spacing of around 0.35 nm. The broad XRD peaks indicate that the as-synthesized materials are composed of nanoparticles, whose corresponding particle sized determined from Scherrer formula is around 6 nm.

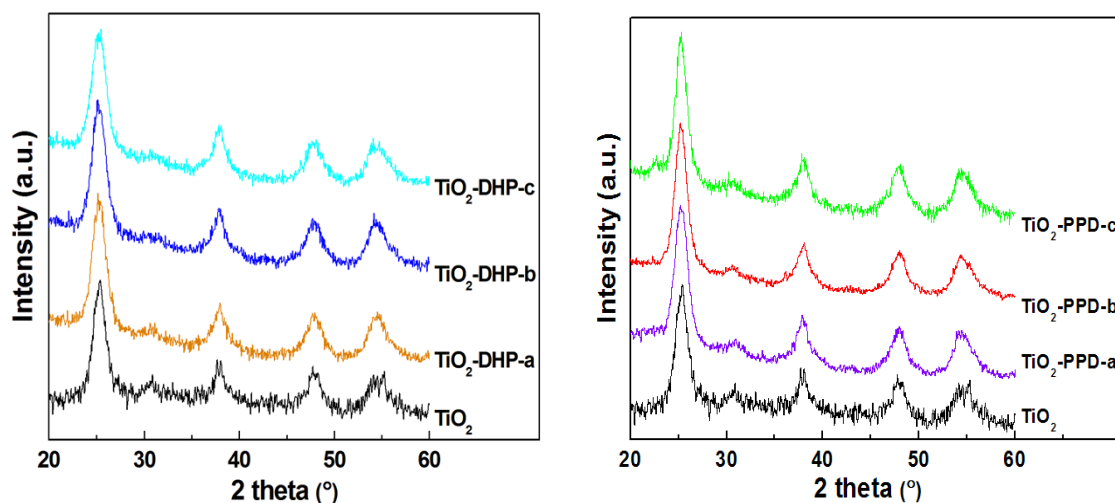


**Figure S5.** Normalized XRD patterns of the TiO<sub>2</sub>-DHP (left) and TiO<sub>2</sub>-PPD (right) organotitanias, as compared to the organic-free mesoporous titania TiO<sub>2</sub>.

TEM analyses of these materials clearly show the mesoporous nature and the crystalline structure of these materials (Figure S6). Spacing of lattice image was determined by using Gatam software and, in all cases, corresponds to 101-spacing of anatase crystalline phase, being the values very similar to those calculated from XRD measurements.

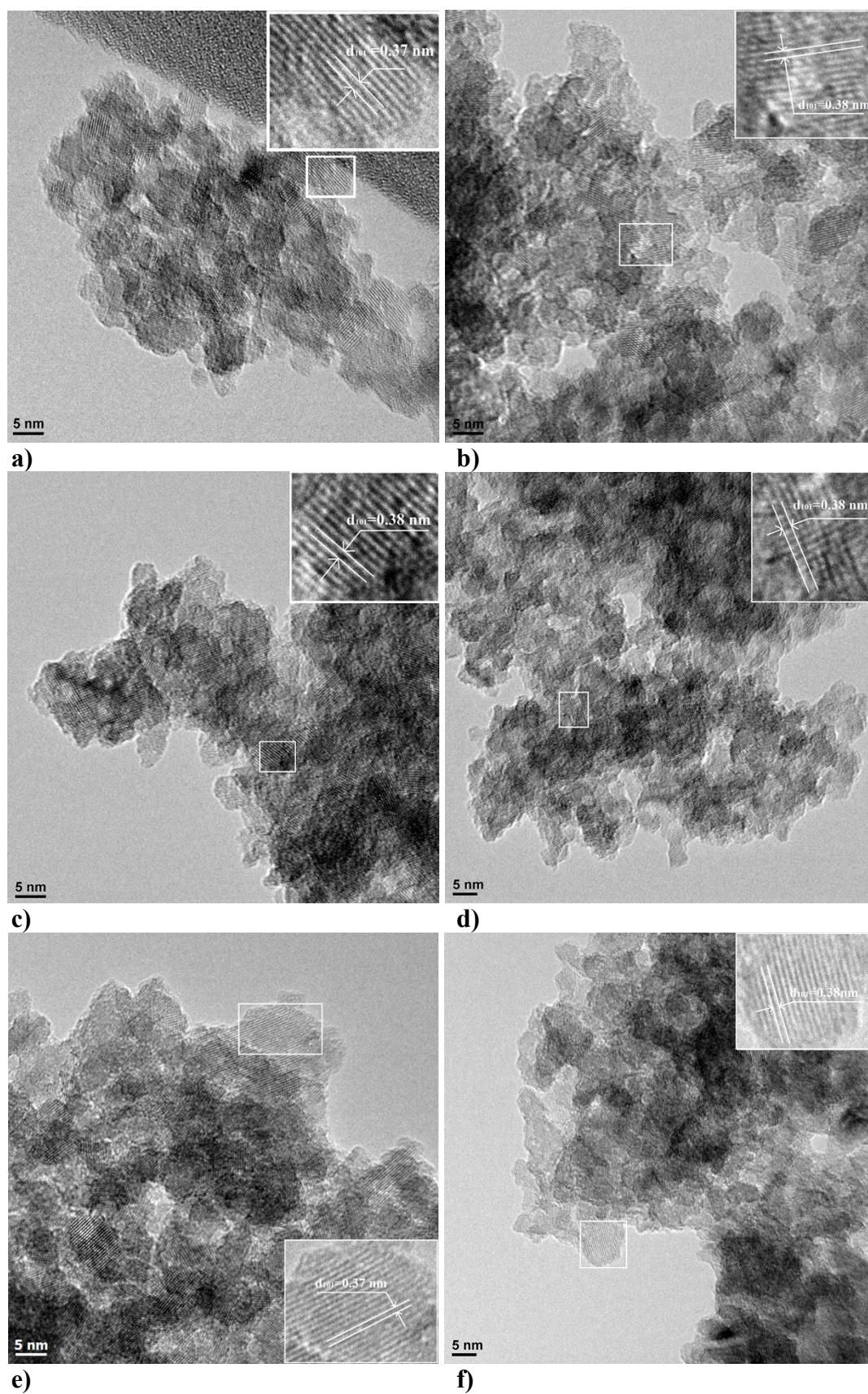


**Figure S6.** TEM images of: (a)  $\text{TiO}_2$ , (b)  $\text{TiO}_2$ -DHP-a, (c)  $\text{TiO}_2$ -DHP-b, (d)  $\text{TiO}_2$ -DHP-c, (e)  $\text{TiO}_2$ -PPD-a and (f)  $\text{TiO}_2$ -PPD-c. Spacing of lattice image was determined by using Gatan software and, in all cases, corresponds to 101-spacing of anatase crystalline phase.



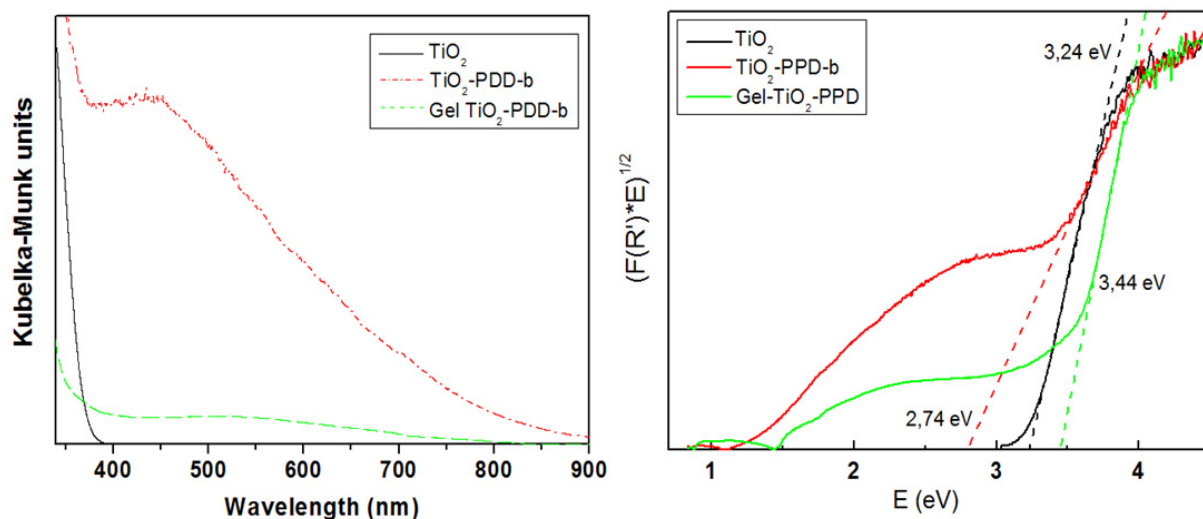


Figure S7. DRUV and Tauc plot of the transformed Kubelka-Munk function versus the energy of light adsorbed of the black titania sample before (pale-grey gel, namely Gel-TiO<sub>2</sub>-PPD-b.) and after the crystallization step (TiO<sub>2</sub>-PPD-b), as compared with the control TiO<sub>2</sub>.

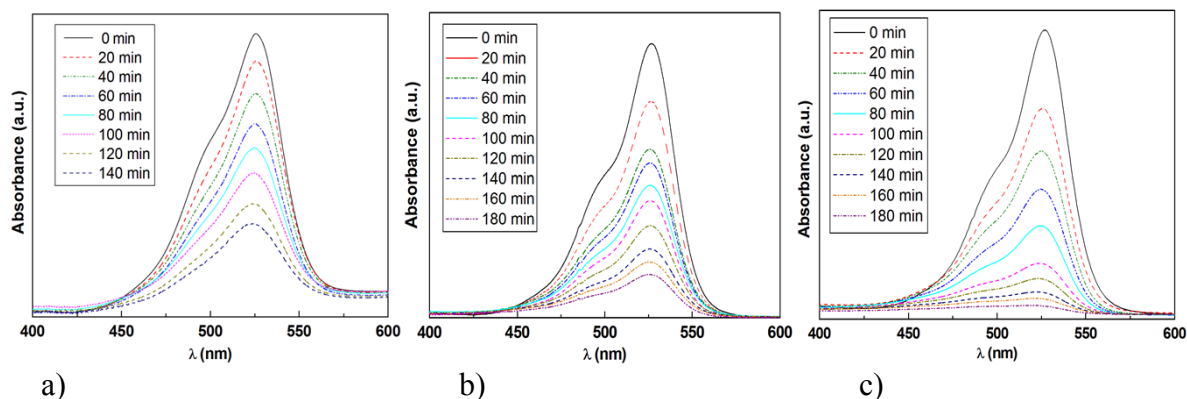


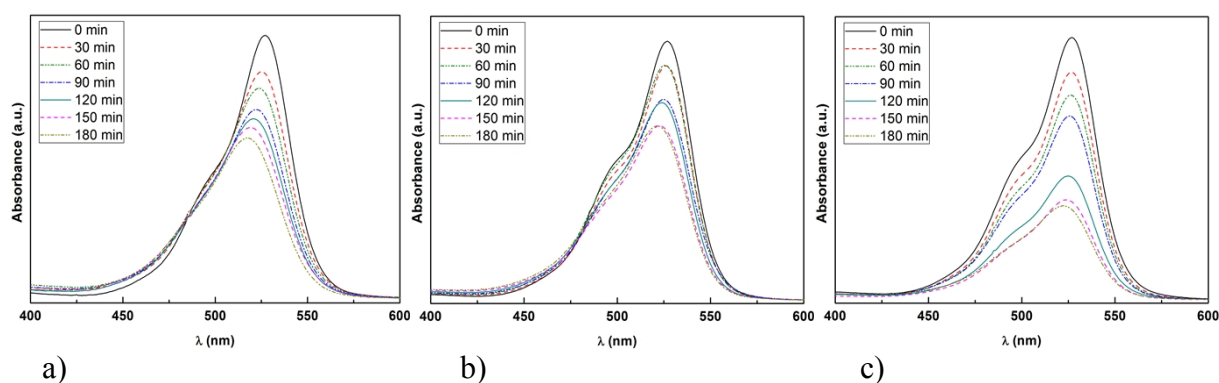
Figure S8. UV-vis absorption spectra of the degradation reaction of an aqueous solution of Rhodamine 6G ( $5 \cdot 10^{-5}$  M) under UV light irradiation using as photocatalysts: (a) TiO<sub>2</sub>, (b) TiO<sub>2</sub>-DHP-b and (c) TiO<sub>2</sub>-PPD-b.



Figure S9. Photographs of the different samples taken along the degradation reaction of an aqueous solution of Rhodamine 6G ( $5 \cdot 10^{-5}$  M) under UV light irradiation using as photocatalysts TiO<sub>2</sub>-PPD-b (left visible illumination, right UV illumination).

TOC measurements of dye adsorption carried out in the absence of light indicated that, after 30 min under stirring, the amount of Rhodamine 6G adsorbed on the TiO<sub>2</sub>-DHP-b catalyst surface was

negligible, while Rhodamine relative concentration diminished up to  $C/C_0 = 0.81 \pm 0.06$  and  $0.69 \pm 0.04$  for control titania and  $\text{TiO}_2\text{-DPH-b}$ , respectively. Thus, the values used for the calculus of mineralization were those measured after 30 min of stirring in absence of light. After 3 h of UV irradiation, carbon concentration decreased by about 40% of the initial concentration when hybrid organotitanias are used as photocatalysts, thus indicating a partial Rhodamine degradation, i.e., no Rhodamine is left in the reaction mixture, but there is still some carbon species in solution. This fact points out that the reaction time for the complete degradation is longer than for complete disappearance of Rhodamine 6G in UV-vis spectra.



**Figure S10.** UV-vis absorption spectra of the degradation reaction of an aqueous solution of Rhodamine 6G ( $5 \times 10^{-5}$  M) under visible light irradiation using as photocatalysts: (a)  $\text{TiO}_2$ , (b)  $\text{TiO}_2\text{-DHP-b}$  and (c)  $\text{TiO}_2\text{-PPD-b}$ .

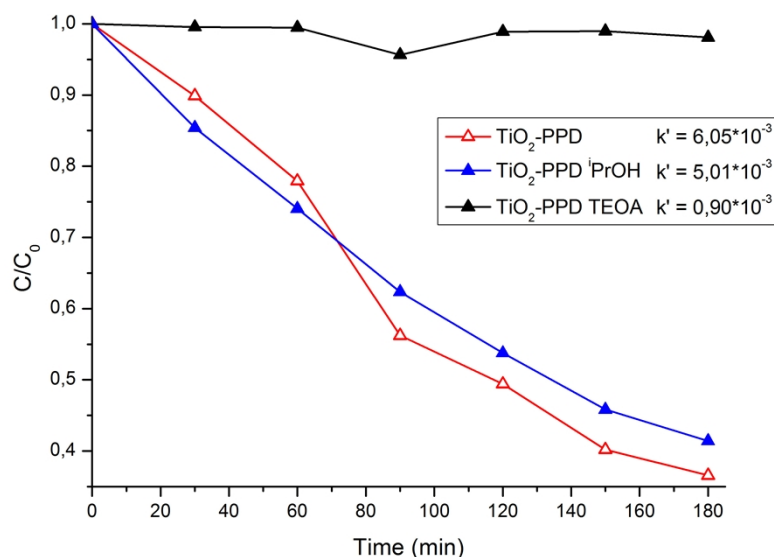


**Figure S11.** Variation of the concentration along the time in the photodegradation reaction of aqueous solutions of R6G ( $5 \times 10^{-5}$  M) by  $\text{TiO}_2\text{-PPD-b}$  in the absence or presence of different scavengers (isopropanol or triethanolamine,  $5 \times 10^{-2}$  M) under visible light irradiation.

## References

[1] C.C. Chusuei, M.A. Brookshier and D.W. Goodman, *Langmuir*, 1999, **15**, 2806.

- [2] P. Kubelka, *J. Opt. Soc. Am.*, 1948, **38**, 448.
- [3] D. Reyes-Coronado, G. Rodriguez-Gattorno, M.E. Espinosa-Pesqueira, C. Cab, R. Coss and G. Oskam, *Nanotechnology*, 2008, **19**, 14605.
- [4] S. Valencia, J.M. Marin and G. Restrepo, *Open Mater. Sci. J.*, 2010, **4**, 9.
- [5] N. Serpone, D. Lawless, and R. Khairutdinovt, *J. Phys. Chem.*, 1995, **99**, 16646.
- [6] L. Zhao and J. Yu, *J. Coll. Int. Sci.*, 2006, **304**, 84.
- [7] A. B. Murphy, *Solar Energy Mater. Solar Cells*, 2007, **91**, 1326
- [8] J. Yu, Q. Li, S. Liu and M. Jaroniec, *Chem. Eur. J.*, 2013, **19**, 2433